The Journal of Neuroscience, May 1, 1996, 16(9):2956–2971

Regulation of α_7 Nicotinic Acetylcholine Receptors in the Developing Rat Somatosensory Cortex by Thalamocortical Afferents

Ron S. Broide,[1] Richard T. Robertson,[2] and Frances M. Leslie[1]

Departments of [1]Pharmacology and [2]Anatomy and Neurobiology, College of Medicine, University of California, Irvine, California 92717

Distributions of α_7 nicotinic acetylcholine receptor (nAChR) mRNA and [^{125}I]α-bungarotoxin (α-BTX) binding sites in the developing rat somatosensory cortex were characterized in relation to acetylcholinesterase (AChE) histochemical staining of thalamocortical terminals to investigate the role of this receptor in cortical development. Using quantitative *in situ* hybridization and receptor autoradiography, elevated levels of mRNA and binding-site expression were first detected at postnatal day 1 (P1) in deep and superficial layers, just beneath the AChE-stained thalamocortical terminals. Onset of expression occurred ~1 d after ingrowth of AChE-stained thalamocortical afferents. By P5, mRNA and binding-site expression exhibited a disjunctive, barrel-like pattern in layer IV and, more clearly, in layer VI. The mRNA and binding-site expressions peaked at ~1 week postnatal and then declined to adult levels. Unilateral electrolytic or cytochemical lesions placed in the thalamic ventrobasal complex at P0 (just as thalamocortical afferents are innervating the cortex) and at P6 (when the somatotopic map is well established) resulted in a marked reduction of α_7 nAChR mRNA and [^{125}I]α-BTX binding-site levels in layers IV and VI, indicating their regulation by thalamocortical afferents. With P6 lesions, this reduction was observed as early as 6 hr postlesion. These results suggest that α_7 nAChRs are localized primarily on cortical cells in rat somatosensory cortex and provide further evidence for thalamocortical influence on cortical ontogeny. These data also suggest a role for cholinergic systems during a critical period of cortical synaptogenesis.

Key words: nicotinic; bungarotoxin; cholinergic; thalamocortical; barrels; cortical development

Considerable attention has been focused on how regions of the neocortex, particularly primary sensory regions, acquire their unique characteristics (Rakic, 1988; O'Leary, 1989). In the rodent, one region of the neocortex that has been studied extensively in relation to this issue is the primary somatosensory cortex (S1). This region contains discrete aggregates of neurons in layer IV known as "barrels" (Woolsey and Van der Loos, 1970), which reflect the pattern of vibrissae on the rodent's face (Killackey and Leshin, 1975). These barrels are innervated by clusters of ventrobasal (VB) thalamic afferents arranged in a somatotopic pattern. Much evidence suggests that early S1 differentiation is strongly influenced by these afferents (for review, see O'Leary et al., 1994).

Numerous studies have analyzed both pre- and postsynaptic markers to determine the earliest appearance of barrel patterns in the S1 (Robertson, 1987; McCandlish et al., 1989; Rhoades et al., 1990; Jhaveri et al., 1991; Paysan et al., 1994). Such studies have demonstrated a periphery-related pattern in the S1 as early as postnatal day 1 (P1). One recent study, examining acetylcholinesterase (AChE) labeling of the developing thalamocortical projection (Schlaggar and O'Leary, 1994), has reported a somatotopic pattern of thalamic terminals in the S1 by birth. This early somatotopic pattern suggests that thalamocortical afferents convey the patterning information to developing S1.

Fuchs (1989) has demonstrated that [^{125}I]α-bungarotoxin (α-BTX) binding exhibits a transient pattern of expression within developing rat sensory cortex. In the S1, this unique columnar pattern is associated with the whisker barrel field in layer IV, but shows a more intense barrel-like expression in layer VI. Several studies have suggested that, in the rat CNS, α-BTX binds to receptors composed of α_7 nicotinic acetylcholine receptor (nAChR) subunits (Alkondon and Albuquerque, 1993; Seguela et al., 1993). We have recently shown a corresponding transient pattern of α_7 nAChR mRNA expression in developing S1, which also exhibits a more intense pattern in layer VI (Broide et al., 1995). This transient pattern of nAChR expression in deeper S1 laminae, coinciding with the period of thalamocortical ingrowth, suggests an intrinsic organization within the cortex that either helps guide innervating afferents or is induced by them.

To address this issue further, we have used quantitative *in situ* hybridization and receptor autoradiography to study the developmental expression of α_7 nAChR mRNA and [^{125}I]α-BTX binding sites in relation to AChE-labeled thalamic terminals in alternate sections from the same brain. We find that thalamocortical afferents appear before the transient pattern of α_7 nAChR distribution. In addition, by interrupting this pathway both at the time that thalamocortical afferents are beginning to innervate the cortex and during a period when the somatotopic map has been well established, we demonstrate a dynamic regulation of α_7 nAChR mRNA and protein levels by thalamocortical afferents. This study provides further evidence for thalamocortical influence on corti-

Received Oct. 10, 1995; revised Jan. 31, 1996; accepted Feb. 5, 1996.

This work was supported by Public Health Service Grant NS30109. We thank Dr. Jim Boulter for providing the α_7 cDNA and Drs. Aric Agmon and Ursula Winzer-Serhan for their comments on this manuscript.

Correspondence should be addressed to Dr. F. M. Leslie, Department of Pharmacology, College of Medicine, University of California, Room 360, MSII, Irvine, CA 92717.

cal development and suggests a possible role for the cholinergic system during this period of synaptogenesis.

MATERIALS AND METHODS

All chemicals were obtained from Sigma (St. Louis, MO) unless otherwise mentioned.

Animals. Timed pregnant Sprague–Dawley rats (Simonsen, Gilroy, CA) were used for this study. Animals were mated during a 2 hr period, and a sperm-positive vaginal smear started embryonic day 0 (E0). Rat pups were born early on E22, and the first 24 hr period after birth was termed P0. Rats aged P0, P1, P2, P3, P5, P7, P10 (n = 6–8 per age), P15, and P70 (n = 4 per age) were used for studying the postnatal time course of α_7 receptor pattern formation. Pups aged P0 were used for young animal lesion studies and allowed to survive for 5 d postlesion (n = 5), whereas pups aged P6 were used for older animal lesion studies and allowed to survive for periods varying from 6 hr to 4 d postlesion (n = 3–4 per time point).

VB thalamic lesions. Rat pups aged P0 were anesthetized by hypothermia, whereas those aged P6 were anesthetized with Metofane (Pitman-Moore, Mundelein, IL). Unilateral lesions of the VB thalamic complex were made using the following coordinates: an anterior–posterior position half the distance between bregma and lambda sutures. For P0 rat pups, 1.5 mm lateral from the medial suture and 3.0 mm ventral from the pial surface. For P6 pups, 2.1–2.3 mm lateral from the medial suture and 3.5–3.7 mm ventral from the pial surface. In 5 P0 animals and 20 P6 animals, the tip of a stainless steel electrode was placed in the VB complex. Electrolytic lesions were made by passing a 0.9 mA positive current for 20 sec. In four P6 animals, the VB received lesions made by injection of 0.25–0.5 μl of 50 mM NMDA. This cytotoxic agent was used because its receptor is one of the earliest glutamatergic receptor subtypes that is expressed in the developing rat thalamus (Laurie and Seeburg, 1994; Monyer et al., 1994). These injections were made using a glass micropipette with a 100 μm beveled tip attached to a 10 μl microsyringe. Animals were sutured and allowed to recover from the anesthetic before being returned to the dam.

Tissue preparation. Rats were decapitated and their brains were quickly removed. Cerebral cortices were separated from the brainstem, flattened between two microscope slides, and then frozen by immersion in isopentane at a temperature below −20°C. These flattened cortices were sectioned tangentially. A tissue block (which included the thalamus) from lesioned brains was frozen and sectioned for lesion verification. In some cases, whole brains were frozen in isopentane at −20°C for 30 sec for cutting in the transverse plane. Brain tissue was stored at −70°C until use. Twenty micrometer tissue sections were cryostat cut and mounted onto either gelatin-coated slides (for [^{125}I]α-BTX binding, AChE histochemistry, or Nissl staining) or slides with an additional coating of poly-L-lysine (for *in situ* hybridization) kept at −20°C. Slide-mounted sections for [^{125}I]α-BTX binding were stored desiccated at 4°C for 2 hr and then stored at −20°C until use. Sections for *in situ* hybridization and AChE staining were post-fixed with 4% paraformaldehyde in 0.1 M PBS, pH 7.4, for 1 hr at 22°C. Sections were then washed in PBS and air dried. Tissue sections for AChE staining were processed immediately, whereas those for *in situ* hybridization were stored desiccated at −20°C until use. Slide-mounted tissue sections for Nissl staining were post-fixed with 10% buffered formalin and stained with cresyl violet.

Probe preparation. A 2.1 kb cDNA encoding the entire rat α_7 nAChR subunit (Genbank accession number M85273) cloned into pBluescript II SK$^+$ was obtained from Dr. Jim Boulter at the Salk Institute, San Diego, CA (Broide et al., 1995). ^{35}S-labeled uridine triphosphate (UTP; Dupont NEN, Boston, MA) was used in synthesizing cRNA riboprobes for *in situ* hybridization. These probes were further subjected to alkaline hydrolysis using the method of Cox et al. (1984) to yield products with average sizes of 600 bases.

In situ *hybridization.* Tissue sections were processed for *in situ* hybridization according to a modification of the method described by Simmons et al. (1989). Briefly, sections were preincubated with 0.1 μg/ml proteinase K (Boehringer Mannheim, Indianapolis, IN) for 10 min at 22°C, acetylated, dehydrated through graded ethanols, and then air dried. Slide-mounted sections were incubated for 18 hr at 60°C with a hybridization solution [50% formamide (Fluka BioChemika, Ronkonkoma, NY), 10% dextran sulfate (Pharmacia, Piscataway, NJ), 0.02% Ficoll, 0.02% polyvinyl pyrolidone, 0.02% bovine serum albumin, 500 μg/ml tRNA, 10 mM dithiothreitol (Boehringer Mannheim), 0.3 M NaCl, 10 mM Tris, pH 8.0, and 1 mM EDTA, pH 8.0] containing cRNA probes labeled with [35S]UTP (Dupont NEN) (1×10^7 cpm/ml) in the antisense orientation. Sections were then incubated with RNase A (20 μg/ml) for 30 min at 37°C, followed by 4 × 5 min high-stringency washes of decreasing salinity (2–0.5× SSC buffer) at 22°C, and a 30 min wash in 0.1× SSC at 70°C. Tissue sections were dehydrated, dried in a stream of cool air, and apposed to β-max film (Amersham, Arlington Heights, IL) for 3 d at 4°C.

[^{125}I]α-BTX binding. Slide-mounted sections for [^{125}I]α-BTX binding were processed according to a modification of the method described by Fuchs (1989). Cortical sections were preincubated in a solution containing 120 mM NaCl and 50 mM Tris-HCl, pH 7.4, for 15 min at 22°C. Slides were then incubated at 22°C for 2 hr in the same buffer containing 5 nM [^{125}I]α-BTX (specific activity >200 Ci/mmol, Amersham). Sections were washed at 4°C in two 10 min buffer rinses followed by 30 sec in distilled water. Tissue sections were dried in a stream of cool air, stored desiccated for 1 d at 22°C, and then apposed to radiation-sensitive Hyperfilm (Amersham) for 4 d.

AChE staining. AChE histochemistry was performed according to a modification of the method of Hedreen et al. (1985). Tissue sections were incubated at 22°C for 10 d in a solution containing 0.132% acetylthiocholine iodide, 50 mM sodium acetate, 0.057 mM tetraisopropylpyrophosphoramide, 2.3 mM copper sulfate, and 2.3 mM copper glycine. Reaction product was then developed by a 15 sec incubation in 1% ammonium sulfide (Fisher Scientific, Pittsburgh, PA).

Data analysis. Autoradiograms were quantified with a computer-based image analysis system (MCID, Imaging Research, St. Catherine, Ontario, Canada) using calibrated standards of reference. A calibration curve of optical density against radioligand concentration (either dpm/mg tissue for *in situ* hybridization or fmol/mg tissue for binding films) was constructed using [^{14}C] brain paste standards of known radioactivity. The curve was calibrated for reading [^{125}I] emissions, as described by Miller and Zahniser (1987). Optical densities in discrete regions of cortical autoradiographic images were measured, and corresponding values of radioactivity were determined by interpolation from the standard curve. The specific activities of cRNA probes used in this study were not determined; therefore, these concentration measurements do not represent the absolute levels of mRNA in the tissue.

Density measurements from the primary barrel cortex were obtained by drawing a border around barrel rows A–E (Woolsey and Van der Loos, 1970). When measuring for partial lesions, only the area affected by the lesion, as evaluated from adjacent AChE-stained sections, was measured. At ages of P5 and older, tangential sections through layer IV were identified as those adjacent to AChE-stained sections showing the barrel-field pattern. Sections through layer VI were identified as those showing the highest density of mRNA and binding levels within the deeper cortical laminae (Broide et al., 1995) and just superficial to the white matter. Other brain regions were identified using the atlas of Paxinos and Watson (1986).

Because cerebral cortex is very thin, tangential tissue sections were conserved for data analysis. Sections were not taken for incubation with sense-oriented riboprobes or with unlabeled competitive drugs for nonspecific binding assessment. Instead, measurements were taken from the perirhinal cortex, adjacent to S1 and auditory cortex, as an internal control in assessing and subtracting background labeling within each experiment. All data were examined by two-way and one-way ANOVA, followed by Newman–Keuls post hoc comparisons.

RESULTS

Emergence of α_7 nAChR pattern in the S1

Transverse sections at the level of the caudate putamen revealed an emerging laminar pattern of α_7 nAChR mRNA and [^{125}I]α-BTX binding-site distribution in the developing S1 (Fig. 1). Two cortical layers exhibited low-to-moderate mRNA and binding-site expression in all cortical regions throughout development. For α_7 nAChR mRNA, these corresponded to the subplate and cell-dense cortical plate, whereas [^{125}I]α-BTX binding-site expression was observed in the subplate and marginal zone, or layer I. These layers, which are present throughout cortical maturation, exhibited a homogeneous expression of mRNA and binding sites when viewed in the tangential plane (data not shown).

The focus of the present investigation, however, was on the emerging cortical layers between the subplate and the cell-dense cortical plate, which exhibited higher mRNA and binding-site expression in

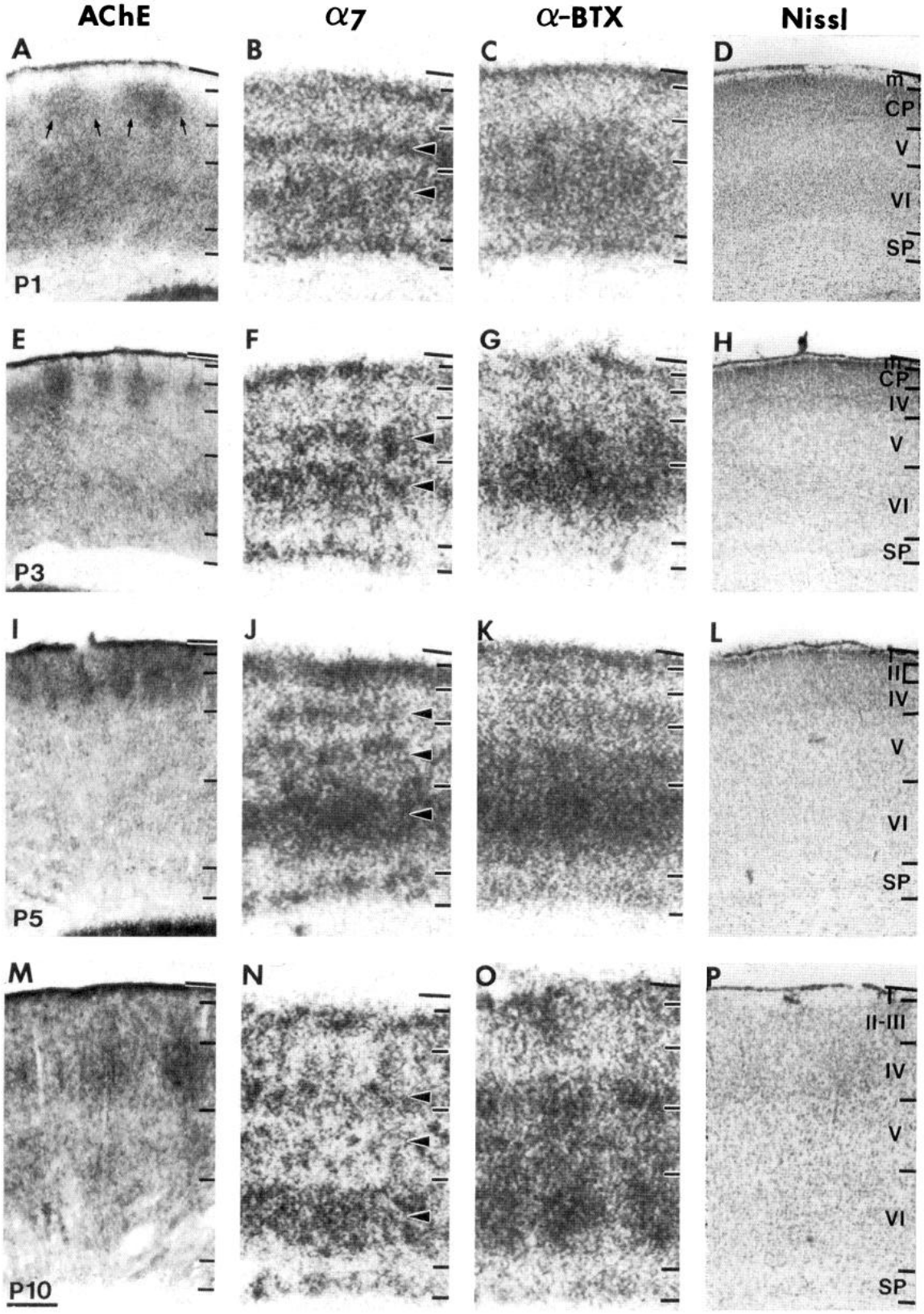

Figure 1. Distributions of AChE-labeled thalamocortical afferents, α_7 nAChR mRNA, and [^{125}I]α-BTX binding sites in the developing S1. Autoradiographic images (α^7 mRNA and *α-BTX* binding sites) and bright-field photomicrographs (*AChE* and *Nissl*) of adjacent series of transverse sections through somatosensory cortex of rats at P1 (*A–D*), P3 (*E–H*), P5 (*I–L*), and P10 (*M–P*). Two clusters of AChE-labeled thalamocortical terminals are indicated at P1 with *small arrows*. *Arrowheads* mark the emerging layers that show a transient distribution of mRNA and binding sites. Positions of cortical layers are indicated on Nissl-stained sections. *SP*, Subplate; *CP*, cortical plate. Scale bar, 300 μm.

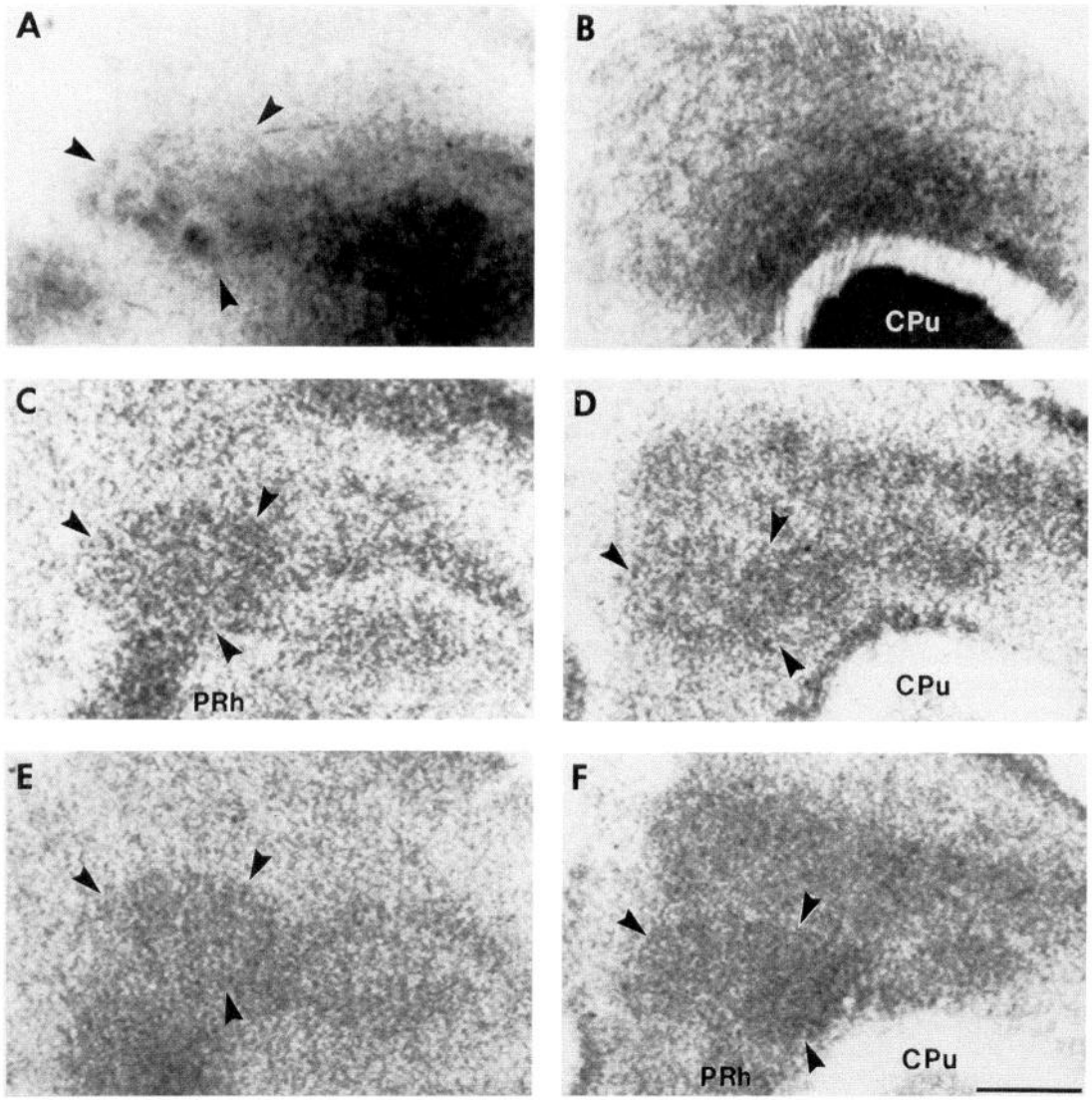

Figure 2. α_7 nAChR mRNA and [^{125}I]α-BTX binding-site distribution in the primary barrel region of superficial and deep laminae of P1 cortex. Tangential sections through the cortex at the level of superficial (*A, C, E*) and deep (*B, D, F*) laminae, showing AChE staining (*A, B*), α_7 mRNA (*C, D*), and [^{125}I]α-BTX binding-site (*E, F*) distributions. The primary barrel region is indicated within *arrowheads*. *CPu*, Caudate putamen; *PRh*, perirhinal cortex. Scale bar, 1 mm.

the S1 than in adjacent cortical regions during development. The complete laminar pattern was observed at ~1 week postnatal. An analysis of individual cortical laminae in the tangential plane also showed the emergence of a somatotopic pattern of mRNA and binding-site expression at corresponding ages (Figs. 2–5).

Postnatal day 0

Transverse sections at P0 revealed AChE-stained thalamocortical terminals at the base of the cortical plate (data not shown). When viewed in the tangential plane, the pattern of these AChE-stained terminals within the S1 appeared disjunctive. In some littermates, higher levels of α_7 nAChR mRNA and [^{125}I]α-BTX binding-site expression were observed in the primary barrel region of the S1 than in adjacent cortical regions (data not shown). However, these patches of higher mRNA and binding expression were not consistently seen in all animals at this age.

Postnatal day 1

At P1, the developing neocortex is comprised of layers VI and V (Fig. 1*D*), with layer IV neurons starting to aggregate at the bottom of the cell-dense cortical plate (Ignacio et al., 1995). Transverse sections at this age revealed AChE-positive thalamocortical afferents localized at the base of the cortical plate (Fig. 1*A*). When viewed in the tangential plane, this AChE staining exhibited a disjunctive pattern (Fig. 2*A*), as previously shown for this age (Schlaggar and O'Leary, 1994). This disjunctive pattern of AChE staining was only observed in superficial layers of the cortex, presumably at the level of the cortical plate, and was not seen in sections of deeper cortical laminae (Fig. 2*B*).

P1 was the earliest age at which levels of α_7 nAChR mRNA and [^{125}I]α-BTX binding-site expression could consistently be detected as higher in the S1 than in adjacent cortical regions. This elevated expression of mRNA and binding was observed clearly within two layers (Fig. 1*B,C*). The laminar boundaries of this S1-specific expression were better defined by mRNA, whereas binding-site expression appeared more evenly distributed across both layers. When compared with the adjacent Nissl-stained section (Fig. 1*D*), the superficial expression was localized to layer V, just below AChE-stained thalamocortical afferents (Fig. 1*A*),

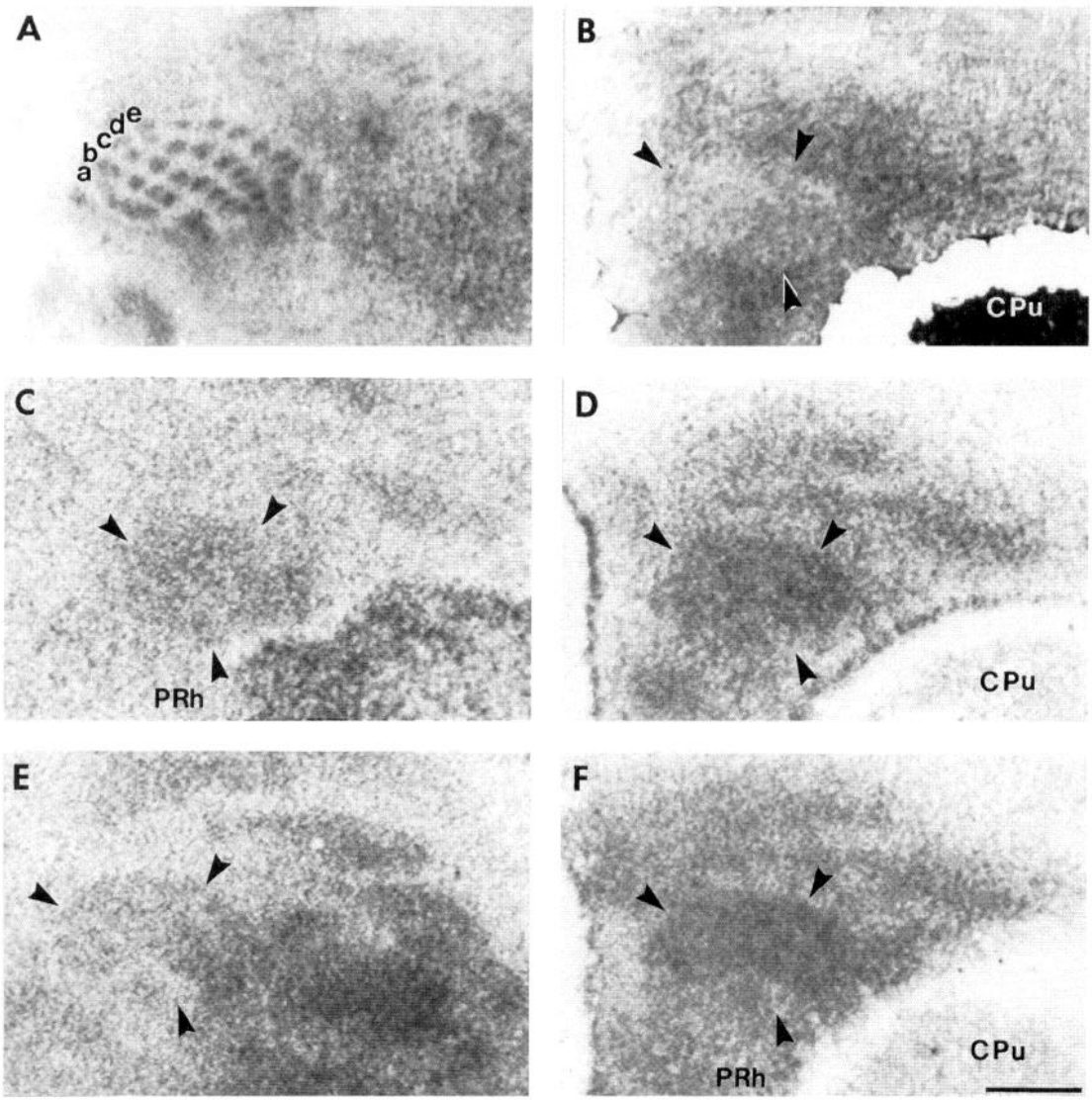

Figure 3. Delineation of the primary barrel region in superficial and deep laminae of P3 cortex by α_7 nAChR mRNA and [^{125}I]α-BTX binding-site expression. Tangential sections through the cortex at the level of superficial (*A, C, E*) and deep (*B, D, F*) laminae, showing AChE staining (*A, B*), α_7 nAChR mRNA (*C, D*), and [^{125}I]α-BTX binding-site (*E, F*) distributions. The primary barrel region (area within *arrowheads*) and the five barrel rows (*a–e*) are indicated. *CPu*, Caudate putamen; *PRh*, perirhinal cortex. Scale bar, 1 mm.

whereas the deeper expression was localized to upper layer VI (Fig. 1*B,C*).

In the tangential plane, an emerging pattern of α_7 nAChR mRNA and [^{125}I]α-BTX binding-site expression, corresponding to the primary barrel region (Fig. 2*C,E*), was detectable in laminae just ventral to the AChE staining pattern (Fig. 2*A*). However, more extensive somatotopic patterns of mRNA and binding-site expression were seen in sections through deeper cortical laminae (Fig. 2*D,F*), which did not exhibit somatotopic AChE staining (Fig. 2*B*). Although the superficial patterns of mRNA and binding sites at this age were in layer V (Fig. 1*A–D*), the deeper patterns were at the level of layer VI, as indicated by the presence of large areas of the caudate (Fig. 2*D,F*) (Broide et al., 1995). At this age, both the mRNA and binding patterns were observed as patches with no apparent further differentiation (Fig. 2*C–F*).

Postnatal day 3

By P3, layer IV has differentiated from the cortical plate (Fig. 1*H*). At this age, AChE-stained thalamic terminals were found distributed mainly in layer IV, with some staining extending into the cortical plate (Fig. 1*E*). The layer IV staining exhibited a distinct barrel pattern when viewed in the tangential plane (Fig. 3*A*). This somatotopic labeling was not visible in deeper cortical sections. Instead, a pattern of slightly negative AChE staining was often observed delineating the primary barrel region within these deeper layers (Fig. 3*B*).

At this age, disjunctive patterns of α_7 nAChR mRNA and [^{125}I]α-BTX binding-site distribution were visible in the primary barrel region. In the transverse plane, laminar patterns of mRNA and binding-site distribution were observed similar to those seen at P1 (Fig. 1*F,G*), with highest levels in layer V and upper layer VI. Although AChE-stained thalamocortical terminals had reached layer IV (Fig. 1*E*), little or no mRNA or binding-site expression was observed in this layer. Tangential sections often exhibited patterns of α_7 nAChR mRNA and [^{125}I]α-BTX binding-site expression in the primary barrel region of superficial (Fig. 3*C,E*) and deep layers (Fig. 3*D,F*) that indicated a subtle row-like

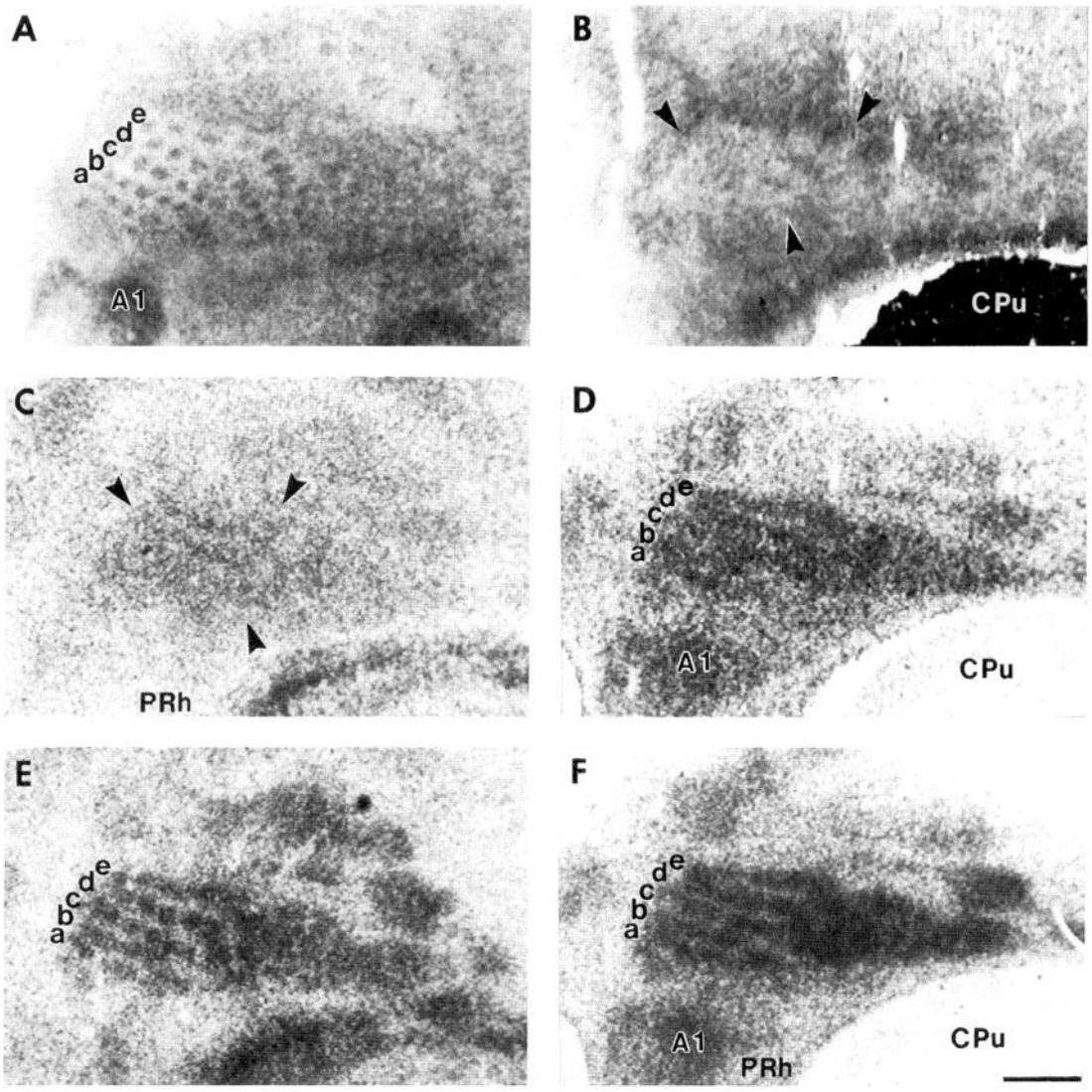

Figure 4. Delineation of the primary barrel region in superficial and deep laminae of P5 cortex by α_7 nAChR mRNA and [^{125}I]α-BTX binding-site expression. Tangential sections through the cortex at the level of superficial (*A, C, E*) and deep (*B, D, F*) laminae, showing AChE staining (*A, B*), α_7 nAChR mRNA (*C, D*), and [^{125}I]α-BTX binding-site (*E, F*) distributions. The primary barrel region (area within *arrowheads*) and the five barrel rows (*a–e*) are indicated. *A1*, Auditory cortex; *CPu*, caudate putamen; *PRh*, perirhinal cortex. Scale bar, 1 mm.

organization. As illustrated in Figure 3, this pattern was better defined by binding (Fig. 3*E,F*) than by mRNA expression (Fig. 3*C,D*).

Postnatal day 5

Layer III could be distinguished from the cortical plate by P5 (Fig. 1*L*). Adjacent transverse sections again showed AChE-positive thalamocortical terminals localized to layer IV and extending into layer III (Fig. 1*I*), whereas a barrel-like distribution of these terminals was seen in the tangential plane (Fig. 4*A*). This AChE-stained pattern was not observed in deeper laminae, but showed a distinct, negative staining pattern of the primary barrel region within layer VI (Fig. 4*B*).

At this age, α_7 nAChR mRNA and [^{125}I]α-BTX binding-site expression was observed in deep layer IV, at the base of AChE-stained thalamic terminals (Fig. 1*J,K*). As in P1 and P3, mRNA and binding-site distribution was still observed in layer V and upper layer VI, with layer VI exhibiting highest levels of expression. In the tangential plane, somatotopic patterns of mRNA and binding-site distribution were clearly detectable in the S1 region (Fig. 4). Although the superficial mRNA pattern was often patchy with limited definition (Fig. 4*C*), the [^{125}I]α-BTX binding pattern was distinctly barrel-like at this level (Fig. 4*E*). These sections were directly adjacent to those exhibiting an AChE-stained barrel pattern (Fig. 4*A*), indicating them to be at the level of layer IV. At the level of layer VI, a more intense barrel-like distribution was evident for both mRNA and binding-site expression (Fig. 4*D,F*). Within layer V, only [^{125}I]α-BTX binding exhibited a barrel-like pattern, but it was faint and lacked the definition observed in layers IV and VI (data not shown).

Postnatal day 10

By P10, all cortical layers can be distinguished in the Nissl-stained section (Fig. 1*P*). Transverse sections through S1 at this age showed clusters of AChE-reactive thalamocortical afferents throughout layer IV and extending slightly into layer III (Fig. 1*M*).

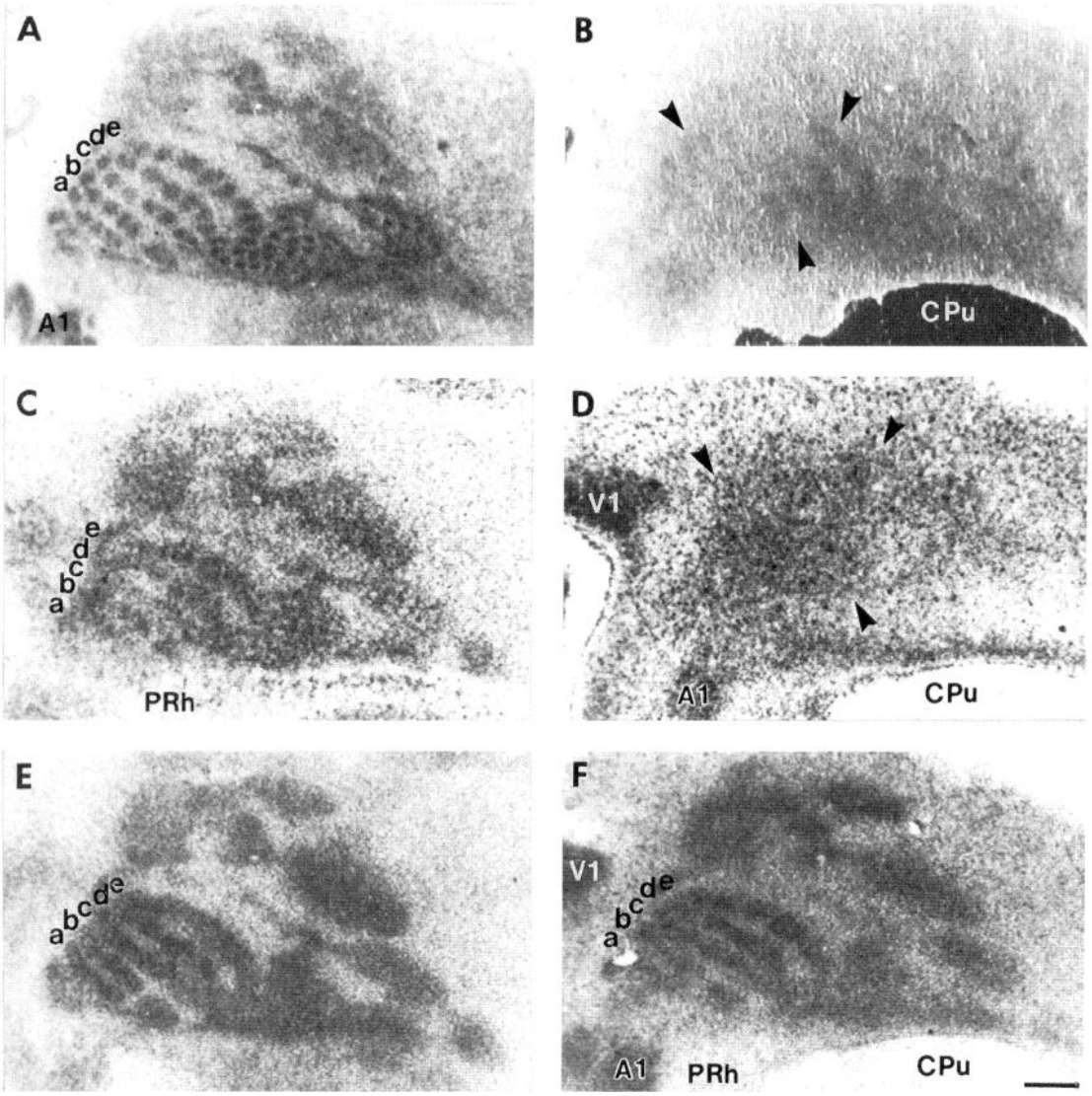

Figure 5. Delineation of the primary barrel region in superficial and deep laminae of P10 cortex by α_7 nAChR mRNA and [^{125}I]α-BTX binding-site expression. Tangential sections through the cortex at the level of superficial (*A, C, E*) and deep (*B, D, F*) laminae, showing AChE staining (*A, B*), α_7 nAChR mRNA (*C, D*), and [^{125}I]α-BTX binding-site (*E, F*) distributions. The primary barrel region (area within *arrowheads*) and the five barrel rows (*a–e*) are indicated. *A1*, Auditory cortex; *CPu*, caudate putamen; *PRh*, perirhinal cortex; *V1*, visual cortex. Scale bar, 1 mm.

In addition, there was some light AChE staining in superficial layer VI and deep layer V. When viewed in the tangential plane of section, an AChE-stained barrel pattern was visible in layer IV (Fig. 5*A*). A similar, but faint AChE staining pattern was also observed in layer VI (Fig. 5*B*).

At this age, mRNA expression was highest in deep layer IV and upper layer VI (Fig. 1*N*). Within layer V, mRNA expression was now diminished and exhibited only scattered cellular labeling. In contrast, [^{125}I]α-BTX binding was distributed in layers IV–VI in a columnar pattern (see Fig. 1O) that corresponded to the pattern of AChE-stained thalamic terminals (Fig. 1*M*). In the tangential plane, barrel patterns of both α_7 mRNA and [^{125}I]α-BTX binding were observed at the level of layer IV (Fig. 5*C,D*). Although most intense in deep layer IV, these patterns spanned the entire layer, corresponding directly to the AChE staining pattern (Fig. 1*M–P*). A barrel-like pattern of [^{125}I]α-BTX binding was also evident within layer VI (Fig. 5*F*); however, the pattern of mRNA expression in this layer was no longer disjunctive. Instead, a patch of mRNA expression slightly higher than in the adjacent cortex was observed (Fig. 5*E*).

Quantitative analysis of α_7 nAChR ontogeny

At P1, the levels of α_7 mRNA and [^{125}I]α-BTX binding in both superficial and deep laminae of S1 were not substantially elevated above surrounding cortex (Fig. 6). By P5, mRNA and binding-site levels in the barrel region exhibited a 200–400% increase in the superficial and deep laminae, with levels in layer VI higher than those in layer IV. Both mRNA and binding in layer VI peaked at P5–P7 and then declined significantly to adult levels ($F_{7,25}$ = 10.698; $F_{7,25}$ = 8.191; $p < 0.0001$; one-way ANOVA). Within layer IV, there was a more delayed peak of mRNA and binding-site expression (Fig. 6), declining after P10 to adult levels ($F_{7,26}$ = 10.435; $F_{7,26}$ = 24.611; $p < 0.0001$; one-way ANOVA). Levels of α_7 nAChR mRNA and [^{125}I]α-BTX binding in the adjacent

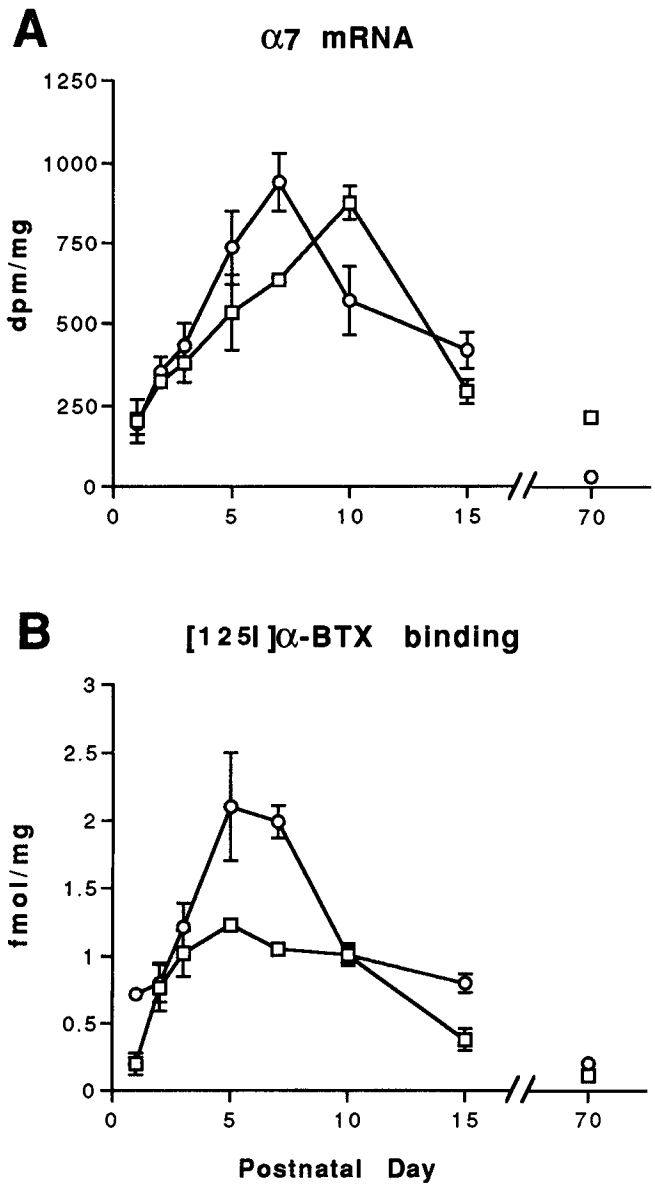

Figure 6. Density of α_7 nAChR mRNA and [^{125}I]α-BTX binding-site expression in the primary barrel region of the somatosensory cortex during postnatal development. The mRNA (*A*) and binding-site (*B*) densities were determined in superficial (*squares*) and deep (*circles*) cortical laminae. Data represent the mean ± SEM for three to six animals.

perirhinal cortex did not show significant changes throughout cortical development (data not shown).

Effects of electrolytic thalamic lesions at P6

To examine the dynamics of regulation by thalamocortical afferents, electrolytic lesions were placed in the VB thalamic complex of P6 animals. After a 6 hr to 4 d survival period, cortical hemispheres were qualitatively and quantitatively analyzed for mRNA and protein expression within the S1. Transverse sections of thalamus were first assessed by light microscopy to verify location and extent of VB lesions. Figure 7*A* shows a unilateral electrolytic lesion of the left VB complex from an animal lesioned on P6 and killed 1 d later. This is an example of a partial lesion, which destroyed the dorsal half of the ventral posterior medial (VPM) and the ventral posterior lateral (VPL) thalamic nuclei. As illustrated in Figure 7*E*, this partial lesion resulted in a loss in AChE-positive staining of rows A–D of the primary barrel field on the ipsilateral cortical hemisphere, while sparing row E and some of row D. The control hemisphere exhibited a normal pattern of AChE staining (Fig. 7*C*).

A similar decline in α_7 nAChR mRNA and [^{125}I]α-BTX binding-site expression in the S1 region of the lesioned hemisphere was observed (Fig. 8). Similar to the pattern of AChE-stained thalamocortical terminals, there was a partial loss in the pattern of mRNA and binding, consistent with the extent of lesion. In both layers IV (Fig. 8*B,F*) and VI (Fig. 8*D,H*), only rows A–D were affected, whereas row E and part of row D were spared. Patterns of expression in the control hemisphere were unaffected (Fig. 8*A,C,E,G*).

Time course of lesion

The loss in AChE staining of thalamocortical terminals within layer IV of the lesioned cortex was not complete until 24 hr postlesion. Animals killed at earlier time points still exhibited an AChE-stained barrel pattern, indicating that thalamic afferents had not completely degenerated (data not shown).

In contrast, quantitative analysis indicated that VB lesions resulted in a 33% decrease in levels of α_7 nAChR mRNA expression in layer IV of the S1 as early as 6 hr postlesion (Fig. 9*A*). By 12 hr postlesion, a maximal 50% reduction was observed that was significantly different from control ($p < 0.05$; Newman–Keuls). There was a slightly delayed reduction in [^{125}I]α-BTX binding (Fig. 9*B*), with a 15% decrease at 12 hr postlesion and a significant 52% reduction at 1 d ($p < 0.05$). By 3 d postlesion, mRNA levels in layer IV of the control and lesioned hemispheres were no longer significantly different and showed an increasing trend, whereas binding-site levels continued to show a significant difference. By the fourth day postlesion, distributions of α_7 nAChR mRNA and [^{125}I]α-BTX binding sites exhibited a somatotopic pattern in layer IV of the lesioned S1, similar to that of control (Fig. 10*C,D,G,H*). However, AChE-labeled thalamic terminals on the lesioned side remained absent at this time period (Fig. 10*A,B*).

In layer VI, a 75% decrease in α_7 nAChR mRNA expression was observed in S1 of the lesioned hemisphere as early as 6 hr postlesion ($p < 0.01$) (Fig. 9*C*), whereas [^{125}I]α-BTX binding-site levels were significantly decreased by 48% at 12 hr postlesion ($p < 0.05$) (Fig. 9*D*). After the first day, levels of mRNA and binding sites in layer VI of the lesioned side showed a significant increase ($F_{5,28} = 2.58$; $F_{5,29} = 3.467$; $p < 0.05$; two-way ANOVA), but remained lower than the control side until the fourth day postlesion. By this time, somatotopic patterns of α_7 nAChR mRNA and [^{125}I]α-BTX binding-site expression were observed to delineate the primary barrel region on the lesioned side, similar to that of control (Fig. 10*E,F,I,J*).

Effects of VB cytochemical lesions

To determine whether the α_7 nAChR mRNA and [^{125}I]α-BTX binding-site loss represented retrograde degeneration of corticothalamic neurons, the VB thalamic complex of P6 animals was injected with NMDA, so that thalamocortical neurons would be killed but corticothalamic projections could be spared. Transverse sections of thalamus were again assessed by light microscopy to verify location and extent of VB lesions. Figure 7*B* shows a unilateral cytochemical lesion of the left VB complex of the thalamus from an animal that survived 1 d postlesion. This was a nearly complete lesion that destroyed both the VPM and VPL as well as the posterior (*Po*) thalamic nuclei. The lesion resulted in a total loss of barrel-like AChE staining in the ipsilateral cortical

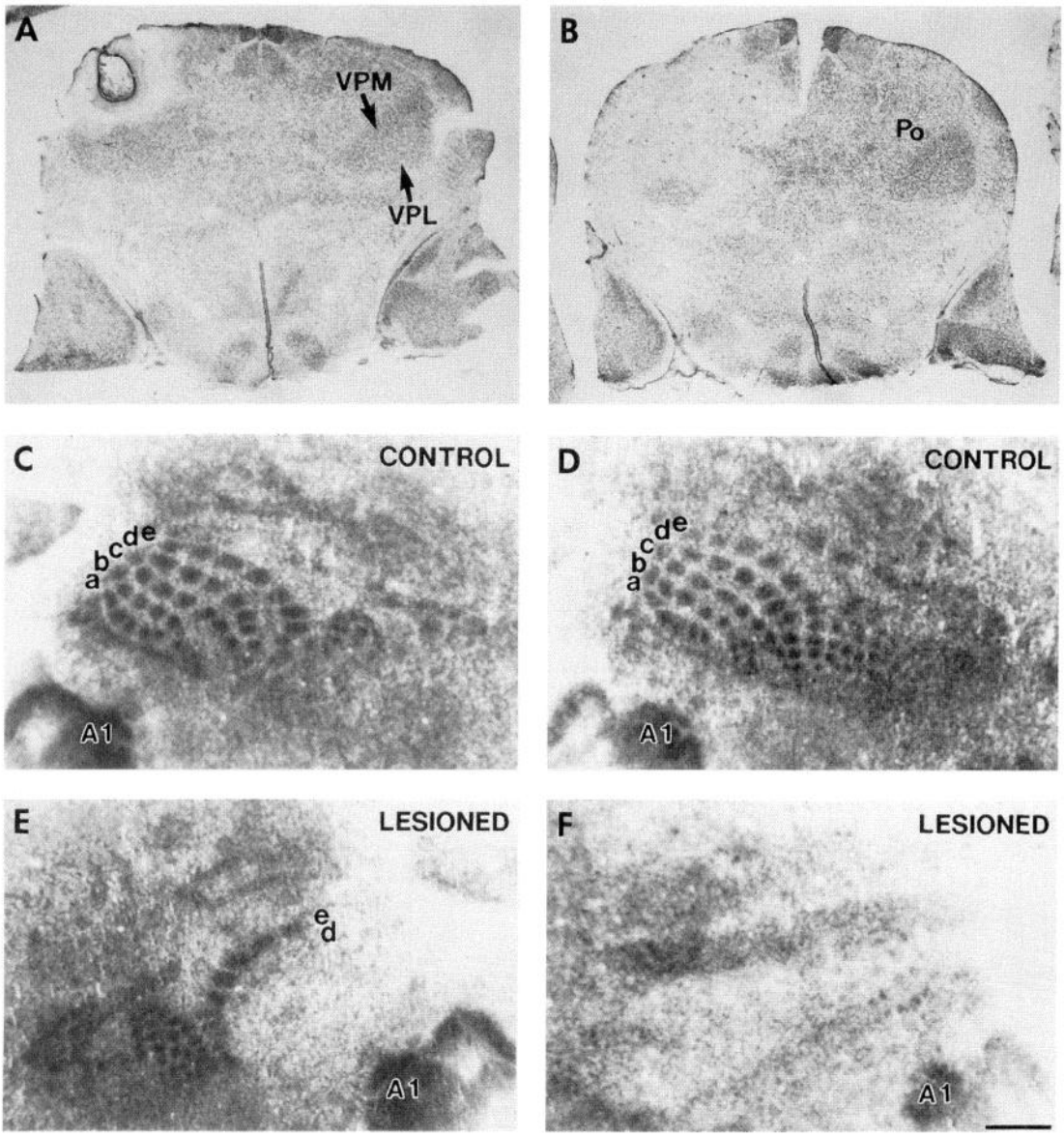

Figure 7. Effects of thalamic lesions on AChE-stained thalamocortical terminals in somatosensory cortex. *A*, Bright-field photomicrograph of a transverse section through the thalamic VB complex, 1 d after placement of a unilateral, electrolytic lesion. Note that only the ventral halves of the ventral posterior medial (*VPM*) and ventral posterior lateral (*VPL*) nuclei are visible in the left hemisphere. *B*, Bright-field photomicrograph of a transverse section through the VB complex, 1 d after placement of a unilateral, cytochemical lesion. Note that most of the VB complex, as well as the posterior thalamic nucleus (*Po*), has been destroyed. *C, E*, Photomicrographs of AChE-stained thalamocortical terminals at the level of layer IV of the control (*C*) and lesioned (*E*) cortical hemispheres from the animal shown in *A*. *D, F*, Photomicrographs of AChE-stained thalamocortical terminals at the level of layer IV of the control (*D*) and lesioned (*F*) hemispheres from the animal shown in *B*. *A1*, Auditory cortex. Scale bar, 1 mm.

hemisphere (Fig. 7*F*), while not affecting terminals on the control side (Fig. 7*D*). A similar decline in α_7 mRNA and [^{125}I]α-BTX binding-site levels was observed in the lesioned cortex (Table 1). Levels of mRNA were decreased by 69% ($p < 0.05$) and 84% ($p < 0.001$), whereas binding levels were decreased by 33% ($p < 0.01$) and 55% ($p < 0.001$) in layers IV and VI, respectively.

Effects of electrolytic thalamic lesions at P0

To examine the influence of thalamocortical innervation on the developmental pattern of α_7 nAChR expression in the S1 cortex, electrolytic lesions were placed in the VB thalamic complex of P0 rat pups. After a 5 d survival, cortical hemispheres were qualitatively and quantitatively analyzed for mRNA and protein expression within the S1. At this age, a barrel-like expression of α_7 mRNA and [^{125}I]α-BTX binding sites within layers IV and VI is clearly visible in the control, unlesioned cortical hemisphere (Fig. 11*C,E,G,I*). Both partial and complete VB lesions resulted in a loss of barrel-like AChE staining in the ipsilateral cortex (Fig. 11*B*), corresponding to the extent of lesion. A similar decline in α_7 nAChR mRNA and [^{125}I]α-BTX binding-site expression in the S1 region of the lesioned hemisphere was observed in layer IV (Fig. 11*D,H*) and layer VI (Fig. 11*F,J*). Levels of mRNA were significantly decreased by 65% ($p < 0.001$) and 79% ($p < 0.001$), whereas binding levels were decreased by 82% ($p < 0.001$) and 81% ($p < 0.001$) in layers IV and VI, respectively (Table 2).

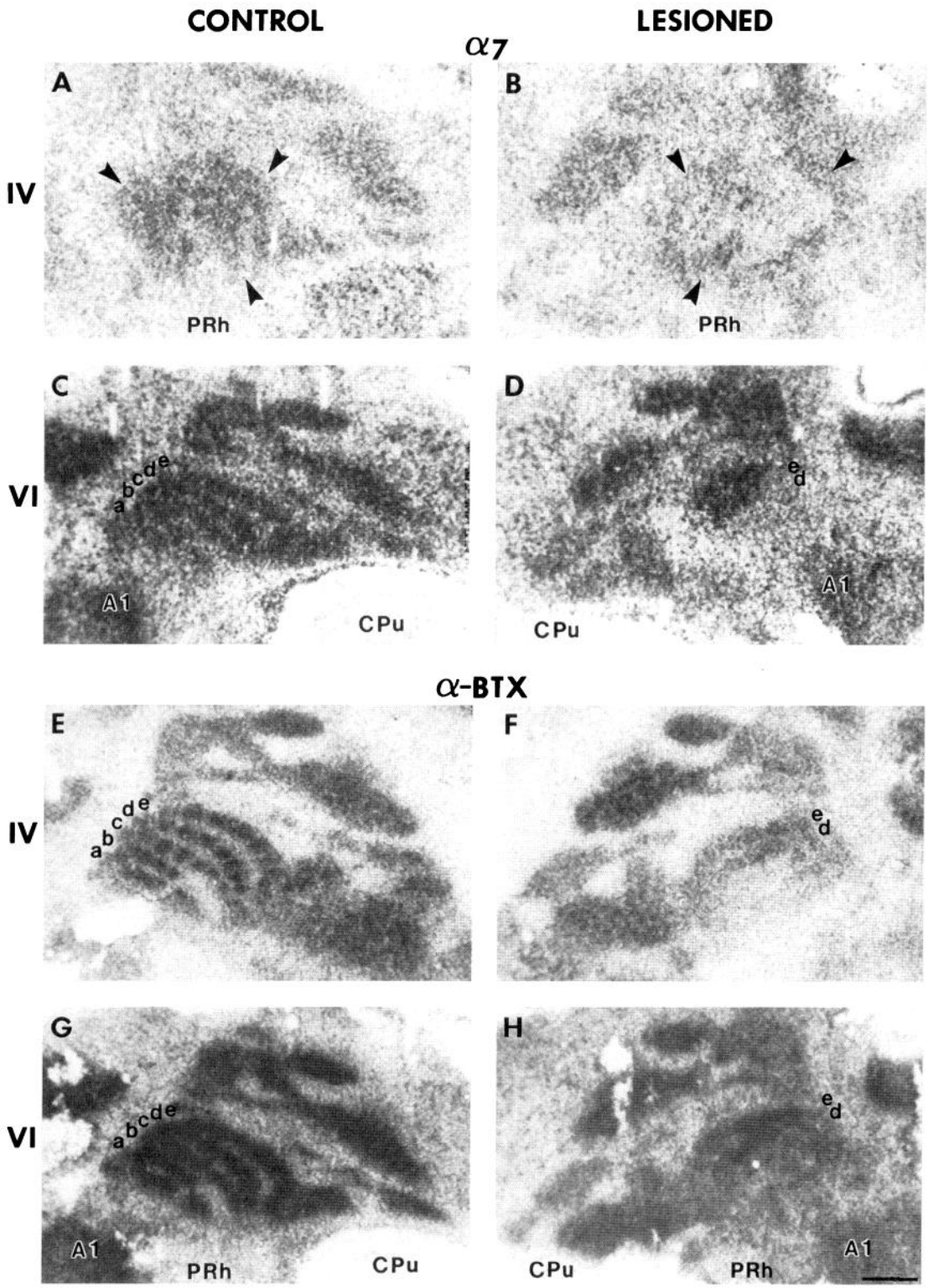

Figure 8. Autoradiographic images of α_7 nAChR mRNA (*A–D*) and [^{125}I]α-BTX binding-site (*E–H*) distributions in the control and lesioned S1 of an animal 1 d after a unilateral, electrolytic lesion at postnatal day 6. Adjacent, tangential sections through the cortex at the level of layers IV (*A, B, E, F*) and VI (*C, D, G, H*). The primary barrel region (area within *arrowheads*) and the five barrel rows (*a–e*) are indicated on the control hemisphere. Note that only rows *d* and *e* of the primary barrel region are visible on the lesioned side. *A1*, Auditory cortex; *CPu*, caudate putamen; *PRh*, perirhinal cortex. Scale bar, 1 mm.

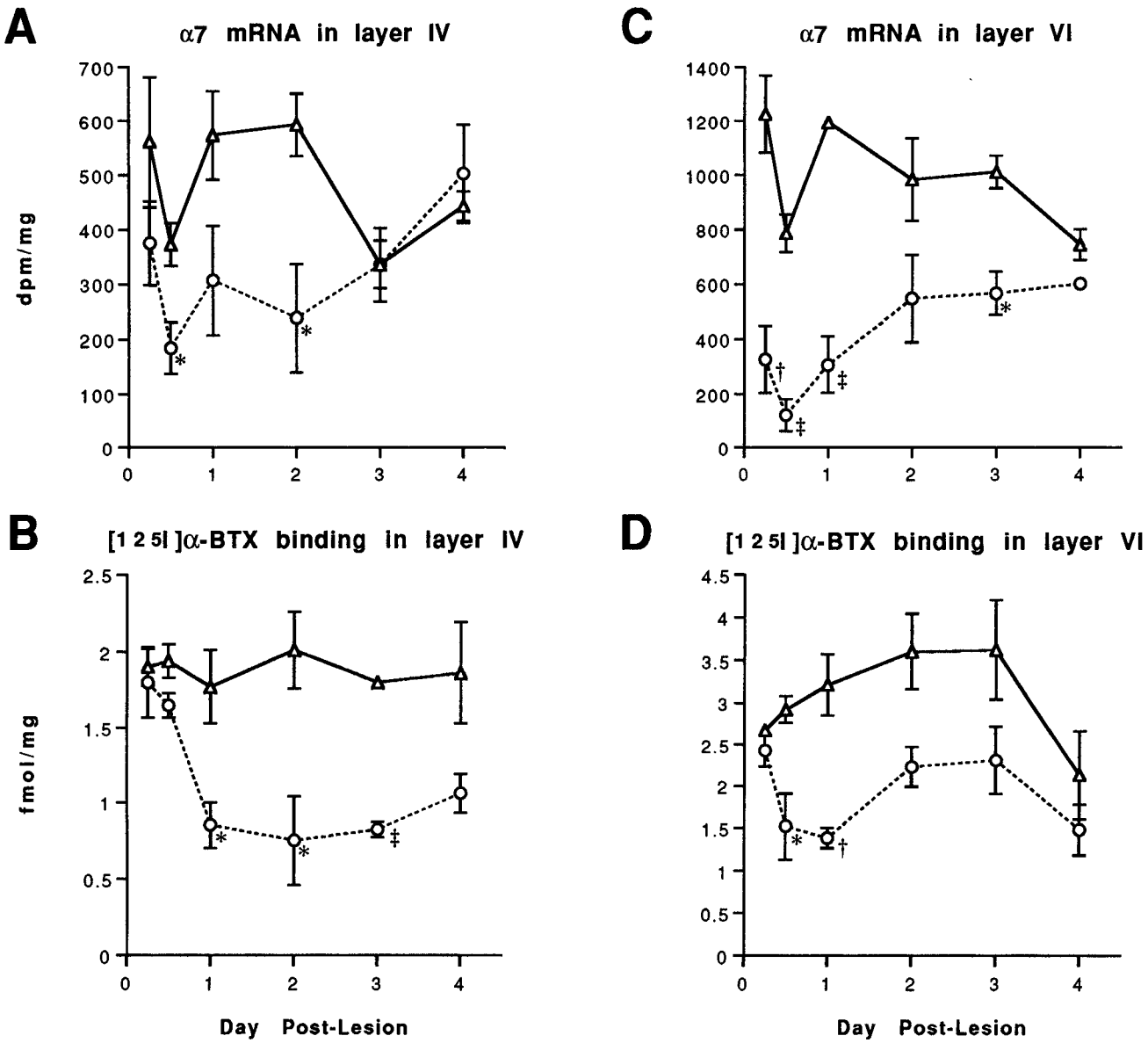

Figure 9. Density of α_7 nAChR mRNA and [^{125}I]α-BTX binding-site expression presented over time for the primary barrel region in the somatosensory cortex of electrolytically lesioned animals. The mRNA (*A, C*) and binding-site (*B, D*) densities were determined at the level of layers IV (*A, B*) and VI (*C, D*) of control (*triangles*) and lesioned (*circles*) hemispheres. Animals received unilateral lesions as described in Materials and Methods. Data represent the mean ± SEM for three to four animals. *, $p < 0.05$, †, $p < 0.01$, ‡, $p < 0.001$ significantly different from the control hemisphere.

Lesion controls

Measurements of α_7 mRNA and [^{125}I]α-BTX binding-site levels in auditory or perirhinal cortex of either electrolytic or cytochemically damaged animals showed no significant difference between the lesioned and control hemispheres (data not shown). In addition, animals that received electrolytic or cytochemical lesions in regions of the thalamus adjacent to VB did not exhibit any decrease in α_7 nAChR mRNA or [^{125}I]α-BTX binding-site levels in the S1. Finally, lesions that affected only a portion of VB affected only corresponding parts of S1.

DISCUSSION

The present study demonstrates transient patterns of α_7 nAChR mRNA and protein expression during the early postnatal period of rat S1 development in deep and superficial laminae. Initial expression occurs ~1 d later than the barrel pattern exhibited by AChE-stained thalamocortical terminals (Schlaggar and O'Leary, 1994). The deeper pattern of receptor expression was localized consistently to upper layer VI, whereas the superficial patterns gradually shifted from deep to more superficial laminae, after the growing thalamocortical axons, and eventually localized in layer IV. Expression peaked at P7–P10 and declined thereafter to adult levels. Placement of lesions in the VB thalamic complex at P0 (just as thalamocortical afferents are innervating the cortex) (Catalano et al., 1991) and at P6 (after the somatotopic map in the S1 has been well established) (Killackey et al., 1995) resulted in a significant decrease in α_7 nAChR mRNA and protein expression in both layers IV and VI of the ipsilateral S1. With P6 lesions, this decline in receptor expression was observed as early as 6 hr postlesion. A complete loss of AChE-stained thalamic terminals, however, was not evident until 1 d postlesion. These data suggest

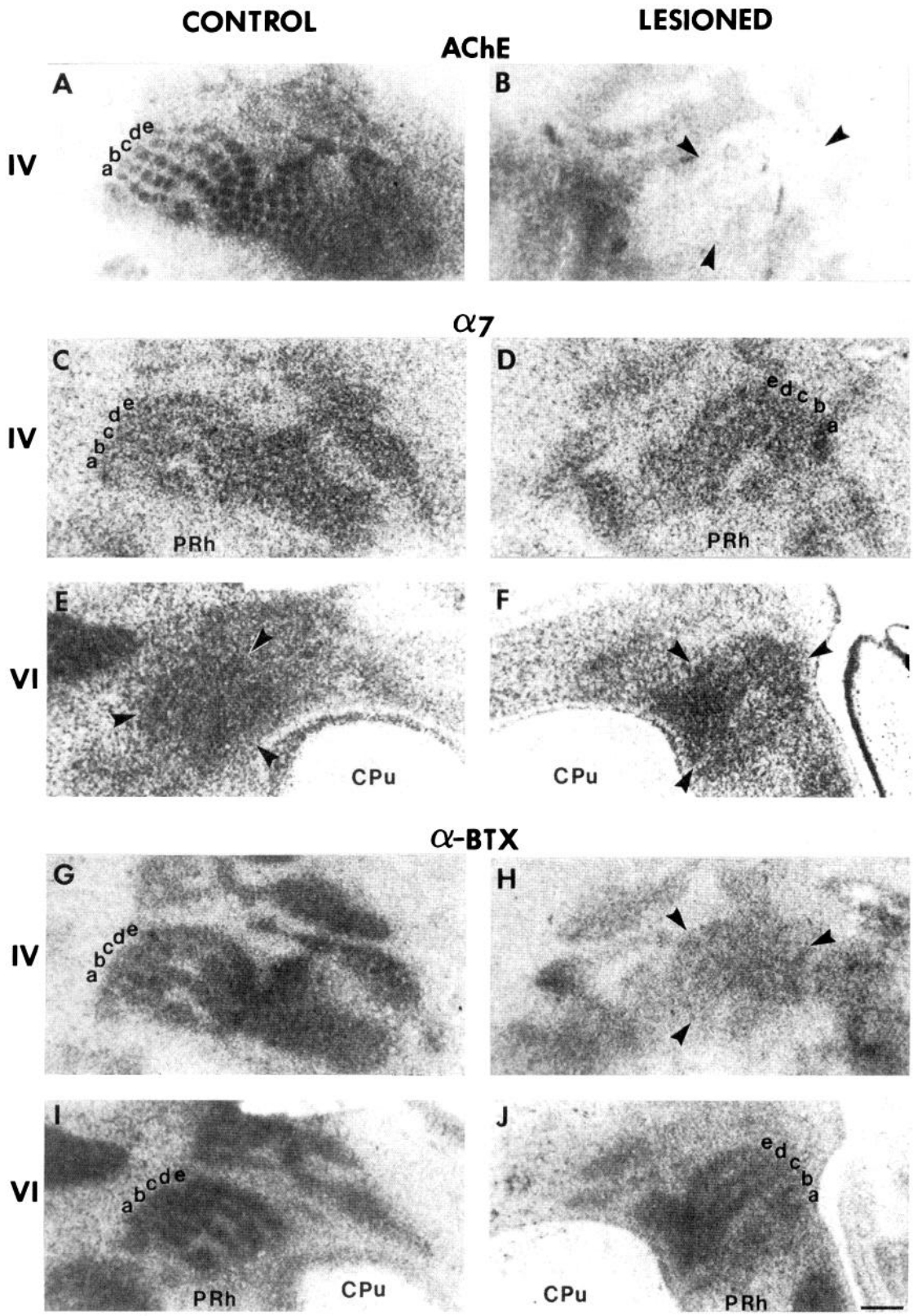

Figure 10. Photomicrographs and autoradiographic images of AChE staining (*A, B*), α_7 mRNA (*C–F*), and [^{125}I]α-BTX binding-site (*G–J*) distributions in the control and lesioned S1 of an animal 4 d after a unilateral, electrolytic lesion at postnatal day 6. Adjacent, tangential sections through the cortex at the level of layers IV (*A, C, E, G, I*) and VI (*B, D, F, H, J*). The primary barrel region (area within *arrowheads*) and the five barrel rows (*a–e*) are indicated. *A1*, Auditory cortex; *CPu*, caudate putamen; *PRh*, perirhinal cortex. Scale bar, 1 mm.

Table 1. Density of α_7 mRNA and [^{125}I]α-BTX binding-site expression in the primary barrel region of P7 pups that received a cytochemical VB lesion at P6

Cortical hemisphere	α_7 mRNA (dpm/mg)		[^{125}I]α-BTX (fmol/mg)	
	IV	VI	IV	VI
Control	487.36 ± 55.93	965.89 ± 49.51	1.53 ± 0.04	1.65 ± 0.11
Lesioned	151.54 ± 85.66*	157.68 ± 68.19‡	1.02 ± 0.09†	0.74 ± 0.04‡

mRNA and binding-site density were determined at the level of layers IV and VI of control and lesioned cortical hemispheres. Animals were unilaterally lesioned on P6 as described in Materials and Methods and allowed to survive for 1 d postlesion. Data represent the mean ± SEM for three to four animals. *, $p < 0.05$, †, $p < 0.01$, ‡, $p < 0.001$ significantly different from the control hemisphere.

a regulation of α_7 nAChRs on cortical neurons in the S1 by thalamocortical afferents.

Methodological issues

Alternate sections from the same brain were processed for AChE histochemistry, α_7 nAChR mRNA expression, and [^{125}I]α-BTX binding. This experimental design was chosen to eliminate inter-animal variability and to permit detailed comparison of the ontogeny of AChE-labeled thalamocortical afferents and α_7 nAChR. Experimental conditions were optimized for receptor analysis and involved the use of cryostat-cut, post-fixed tissue sections. Standard AChE processing conditions were appropriately modified to allow visualization of signal in nonperfused tissue. Although not optimized for enzymatic analysis, the developmental pattern of AChE that was observed is similar to that reported by Schlaggar and O'Leary (1994).

To conserve tissue, sections for receptor analysis were not processed for nonspecific binding or sense hybridization. Previous studies from our laboratory have shown that nonspecific binding or hybridization represents <35% and 6% of total signal in this region, respectively (Broide et al., 1995). Rather than use separate sections as nonspecific controls, labeling within the perirhinal cortex region of the experimental section was measured and subtracted as background, since labeling within this region did not change significantly with age or lesion.

Ontogeny of α_7 nAChRs in relation to thalamic afferents

Whereas layer VI of S1 is labeled by AChE at P0, consistent expression of α_7 nAChRs was not observed in this region until P1. Our observation that α_7 receptor expression follows the pattern delineated first by AChE suggests that expression of α_7 nAChRs in the S1 may be induced by ingrowing thalamocortical afferents.

One feature of α_7 nAChR expression in developing S1 is the somatotopic representation observed in both deep and superficial laminae. Whereas the deep pattern is consistently observed in layer VIa, a superficial pattern develops behind ingrowing thalamocortical terminals. In the lower tier, the barrel patterns of α_7 nAChR mRNA and protein expression become clearly evident at P3–P5. Earlier studies have demonstrated that ingrowing thalamocortical axons arborize in this region in a somatotopic pattern (Agmon et al., 1993; Schlaggar and O'Leary, 1994). The consistent feature in our data is that growing thalamocortical axons appear organized in a somatotopic pattern in deeper layers and eventually in layer IV, and that a somatotopic pattern of α_7 nAChR mRNA and [^{125}I]α-BTX binding appears to follow the thalamocortical pattern by ~1 d.

Effects of thalamic lesions

Our lesion data have confirmed the critical influence of ingrowing thalamocortical afferents on α_7 nAChR expression in layers IV and VI. Electrolytic ablation of neurons in the thalamic VB nucleus of P6 rat pups, after the somatotopic map in the S1 has been well established, results in a rapid loss of α_7 nAChR expression in both cortical layers. The loss in α_7 mRNA expression is maximally decreased within 12 hr postlesion before the disappearance of AChE labeling of thalamocortical terminals. A corresponding but slightly delayed loss of protein is maximal within 24 hr. Cytochemical lesions of the VB at P6 also result in a significant and rapid decline in mRNA and protein expression in both layers IV and VI, confirming the specificity of this effect and eliminating the possible involvement of the reciprocal corticofugal pathway, which develops in parallel with the thalamocortical axons (De Carlos and O'Leary, 1992; Miller et al., 1993).

After the initial downregulation after P6 lesions, however, some recovery of α_7 nAChR expression is observed such that with longer postlesion periods, the differences between control and lesion sides are no longer statistically significant. Furthermore, there is some re-emergence of the somatotopic pattern in both layers even though the loss of AChE-labeled terminals is complete. Thus, after the critical period of cortical development, α_7 nAChR expression is dynamically modulated and not completely dependent on thalamocortical innervation.

Electrolytic lesions placed in the VB of P0 pups at the time when thalamocortical afferents are just beginning to innervate the cortex results in a lack of the normal α_7 nAChR developmental pattern in layers IV and VI of the ipsilateral S1. These results suggest that during the critical period of cortical development, ontogeny of α_7 nAChR expression is dependent on thalamocortical innervation. Taken together, these lesion data indicate that there is a very tight coupling between the thalamocortical pathway and cortical α_7 nAChR expression, and further suggest that these ingrowing afferents imprint a somatotopic pattern in both layers IV and VI.

The rapid loss of radioligand binding observed after placement of lesions may indicate a very rapid turnover of receptor protein. A high rate of turnover of peripheral nAChRs has previously been observed at the developing neuromuscular junction (Michler and Sakmann, 1980; Reiness and Weinberg, 1981). Alternatively, the observed binding changes may reflect alterations in receptor affinity or rapid internalization to an intracellular receptor pool (Stollberg and Berg, 1987).

Evidence for α_7 nAChRs on thalamocortical afferents

Our present data suggest that α_7 nAChRs in developing S1 are localized primarily to cortical cells. However, in rat, α_7 mRNA is also expressed in the VB thalamic complex (Broide et al., 1995), which could suggest that a proportion of α_7 nAChR expression in layer IV is on presynaptic terminals. Consistent with this hypothesis is our observation that the pattern of protein expression in layer IV is more discrete than that of mRNA. However, the

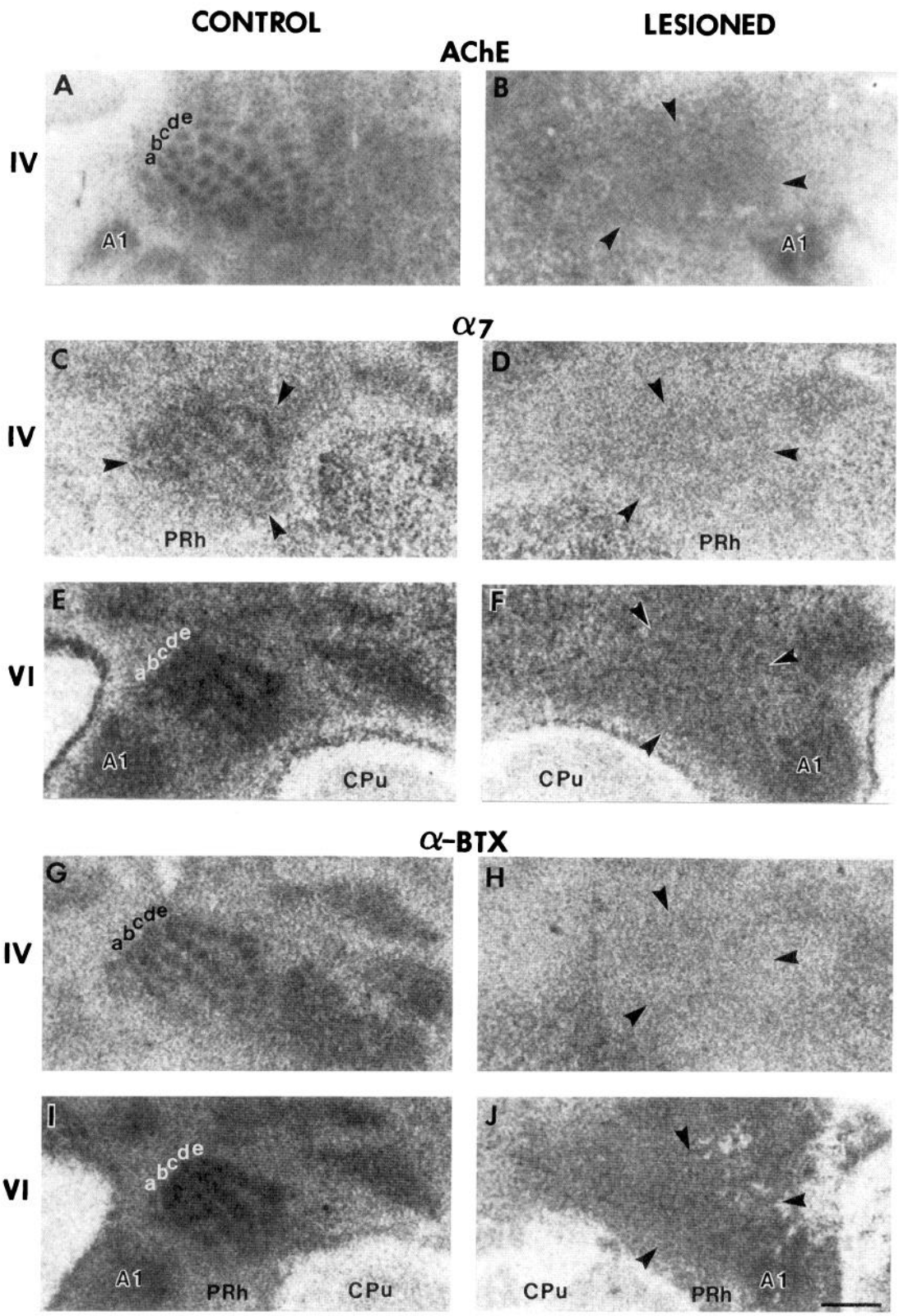

Figure 11. Photomicrographs and autoradiographic images of AChE staining (*A, B*), α_7 mRNA (*C–F*), and [^{125}I]α-BTX binding-site (*G–J*) distributions in the control and lesioned S1 of an animal 5 d after a unilateral, electrolytic lesion at postnatal day 0. Adjacent, tangential sections through the cortex at the level of layers IV (*A, C, E, G, I*) and VI (*B, D, F, H, J*). The primary barrel region (area within *arrowheads*) and the five barrel rows (*a–e*) are indicated. *A1*, Auditory cortex; *CPu*, caudate putamen; *PRh*, perirhinal cortex. Scale bar, 1 mm.

Table 2. Density of α_7 mRNA and [^{125}I]α-BTX binding-site expression in the primary barrel region of P5 pups that received an electrolytic VB lesion at P0

Cortical hemisphere	α_7 mRNA (dpm/mg)		[^{125}I]α-BTX (fmol/mg)	
	IV	VI	IV	VI
Control	321.86 ± 26.53	728.28 ± 61.33	0.94 ± 0.05	1.54 ± 0.15
Lesioned	112.54 ± 16.39‡	153.83 ± 33.21‡	0.17 ± 0.08‡	0.29 ± 0.17‡

mRNA and binding-site density were determined at the level of layers IV and VI of control and lesioned cortical hemispheres. Animals were unilaterally lesioned on P0 as described in Materials and Methods and allowed to survive for 5 d postlesion. Data represent the mean ± SEM for five animals. ‡, $p < 0.001$ significantly different from the control hemisphere.

ontogeny of protein expression in layer IV is later than that of AChE-labeled thalamic afferents and is more consistent temporally with the expression of mRNA in this region. Electron microscopic studies will be required to further clarify this issue.

Role of α_7 nAChRs in S1 ontogeny

Much recent data implicate the α_7 nAChR in mechanisms underlying cellular plasticity. Previous studies have shown this receptor to be developmentally regulated (Couturier et al., 1990; Broide et al., 1995) and that activation of this receptor induces Ca^{2+} influx (Vijayaraghavan et al., 1992; Seguela et al., 1993; Zhang et al., 1994) and subsequent neurite retraction (Chan and Quik, 1993; Pugh and Berg, 1994). Thus, the transient expression during the critical period of rat S1 development is consistent with a developmental role in establishing cortical circuitry.

For this hypothesis to be valid, there must be a source of endogenous ACh within cortex during this period of early postnatal development. A transient expression of cholinergic neurons within rat sensory cortex has been reported to peak during the perinatal period (Dori and Parnavelas, 1989). Also, cortical ingrowth of basal forebrain afferents in this species has been observed as early as P0 (Calarco and Robertson, 1995). DiI-labeling studies have indicated that early postnatal development of basal forebrain fibers coincides temporally with the expression of α_7 nAChRs, which we document in the present study. Whereas ChAT expression in these basal forebrain afferents has not been detected before P5 (Kiss and Patel, 1992), the cells of origin are ChAT-positive at the time of birth (Gould et al., 1991). It is therefore possible that ACh may be released from basal forebrain axons during early postnatal development. Electrophysiological studies will be required to address this issue further.

Our present data, indicating expression of a cholinergic receptor in association with AChE-labeled thalamocortical afferents, suggest the possibility that functional cholinergic synapses may exist during this critical period of cortical development. Thus, a functional triad may be formed between basal forebrain afferents, thalamocortical afferents, and cortical target cells. If, as extensive literature suggests (O'Leary et al., 1994), thalamocortical afferents stimulate differentiation of cortical structure and function, the α_7 nAChR may serve as an early transducer of this process.

REFERENCES

Agmon A, Yang LT, O'Dowd DK, Jones EG (1993) Organized growth of thalamocortical axons from the deep tier of terminations into layer IV of mouse barrel cortex. J Neurosci 13:5365–5382.

Alkondon M, Albuquerque EX (1993) Diversity of nicotinic acetylcholine receptors in rat hippocampal neurons. I. Pharmacological and functional evidence for distinct structural subtypes. J Pharmacol Exp Ther 265:1455–1473.

Broide RS, O'Connor LT, Smith MA, Smith JAM, Leslie FM (1995) Developmental expression of α_7 neuronal nicotinic receptor messenger RNA in rat sensory cortex and thalamus. Neuroscience 67:83–94.

Calarco CA, Robertson RT (1995) Development of basal forebrain projections to visual cortex: DiI studies in rat. J Comp Neurol 354:608–626.

Catalano SM, Robertson RT, Killackey HP (1991) Early ingrowth of thalamocortical afferents to the neocortex of the prenatal rat. Proc Natl Acad Sci USA 88:2999–3003.

Chan J, Quik M (1993) A role for the nicotinic α-bungarotoxin receptor in neurite outgrowth in PC12 cells. Neuroscience 56:441–451.

Couturier S, Bertrand D, Matter JM, Hernandez MC, Bertrand S, Millar N, Valera S, Barkas T, Ballivet M (1990) A neuronal nicotinic acetylcholine receptor subunit (α_7) is developmentally regulated and forms a homo-oligomeric channel blocked by α-BTX. Neuron 5:847–856.

Cox KH, DeLeon DV, Angerer LM, Angerer RC (1984) Detection of mRNAs in sea urchin embryos by *in situ* hybridization using asymmetric RNA probes. Dev Biol 101:485–502.

De Carlos JA, O'Leary DDM (1992) Growth and targeting of subplate axons and establishment of major cortical pathways. J Neurosci 12:1194–1211.

Dori I, Parnavelas JG (1989) The development of basal forebrain projections to the rat visual cortex. Exp Brain Res 76:563–571.

Fuchs JL (1989) [^{125}I]α-Bungarotoxin binding marks primary sensory areas of developing rat neocortex. Brain Res 501:223–234.

Gould E, Woolf NJ, Butcher LL (1991) Postnatal development of cholinergic neurons in the rat: I. Forebrain. Brain Res Bull 27:767–789.

Hedreen JC, Bacon SJ, Price DL (1985) A modified histochemical technique to visualize acetylcholinesterase-containing axons. J Histochem Cytochem 33:134–140.

Ignacio MPD, Kimm EJ, Kageyama GH, Yu J, Robertson RT (1995) Postnatal migration of neurons and formation of laminae in rat cerebral cortex. Anat Embryol (Berl) 191:89–100.

Jhaveri S, Erzurumlu RS, Crossin K (1991) Barrel construction in rodent neocortex: role of thalamic afferents versus extracellular matrix molecules. Proc Natl Acad Sci USA 88:4489–4493.

Killackey HP, Leshin S (1975) The organization of specific thalamocortical projections to the posteromedial barrel subfield of the rat somatic sensory cortex. Brain Res 86:469–472.

Killackey HP, Rhoades RW, Bennett-Clarke CA (1995) The formation of a cortical somatotopic map. Trends Neurosci 18:402–407.

Kiss J, Patel AJ (1992) Development of the cholinergic fibres innervating the cerebral cortex of the rat. Int J Dev Neurosci 10:153–170.

Laurie DJ, Seeburg PH (1994) Regional and developmental heterogeneity in splicing of the rat brain NMDAR1 mRNA. J Neurosci 14:3180–3194.

McCandlish C, Waters RS, Cooper NGF (1989) Early development of the representation of the body surface in S1 cortex barrelfield in neonatal rats as demonstrated with peanut agglutinin binding: evidence for differential development within the rattunculus. Exp Brain Res 77:425–431.

Michler A, Sakmann B (1980) Receptor stability and channel conversion in the subsynaptic membrane of the developing mammalian neuromuscular junction. Dev Biol 80:1–17.

Miller JA, Zahniser NR (1987) The use of ^{14}C-labeled tissue paste standards for the calibration of ^{125}I-labeled ligands in quantitative autoradiography. Neurosci Lett 81:345–350.

Miller B, Chou L, Finlay BL (1993) The early development of thalamocortical and corticothalamic projections. J Comp Neurol 335:16–41.

Monyer H, Burnashev N, Laurie DL, Sakmann B, Seeburg PH (1994) Developmental and regional expression in the rat brain and functional properties of four NMDA receptors. Neuron 12:529–540.

O'Leary DDM (1989) Do cortical areas emerge from a protocortex? Trends Neurosci 12:400–406.

O'Leary DDM, Schlaggar BL, Tuttle R (1994) Specification of neocortical areas and thalamocortical connections. Annu Rev Neurosci 17:419–439.

Paxinos G, Watson C (1986) The rat brain in stereotaxic coordinates. Sydney: Academic.

Paysan J, Bolz J, Mohler H, Fritschy J-M (1994) $GABA_A$ receptor α_1 subunit, an early marker for area specification in developing rat cerebral cortex. J Comp Neurol 350:133–149.

Pugh PC, Berg DK (1994) Neuronal acetylcholine receptors that bind α-bungarotoxin mediate neurite retraction in a calcium-dependent manner. J Neurosci 14:889–896.

Rakic P (1988) Specification of cerebral cortical areas. Science 241:170–176.

Reiness CG, Weinberg CB (1981) Metabolic stabilization of acetylcholine receptors at newly formed neuromuscular junctions in rat. Dev Biol 84:247–254.

Rhoades RW, Bennett-Clarke CA, Chiaia NL, White FA, Macdonald GJ, Haring JH, Jacquin MF (1990) Development and lesion induced reorganization of the cortical representation of the rat's body surface as revealed by immunocytochemistry for serotonin. J Comp Neurol 293:190–207.

Robertson RT (1987) A morphogenic role for transiently expressed acetylcholinesterase in developing thalamocortical systems? Neurosci Lett 75:259–264.

Schlaggar BL, O'Leary DDM (1994) Early development of the somatotopic map and barrel patterning in rat somatosensory cortex. J Comp Neurol 346:80–96.

Seguela P, Wadiche J, Dineley-Miller K, Dani JA, Patrick JW (1993) Molecular cloning, functional properties, and distribution of rat brain α_7: a nicotinic cation channel highly permeable to calcium. J Neurosci 13:596–604.

Simmons DM, Arriza JL, Swanson LW (1989) A complete protocol for *in situ* hybridization of messenger RNAs in brain and other tissues with radiolabeled single-stranded RNA probes. J Histotechnol 12:169–181.

Stollberg J, Berg DK (1987) Neuronal acetylcholine receptors: fate of surface and internal pools in cell culture. J Neurosci 7:1809–1815.

Vijayaraghavan S, Pugh PC, Zhang ZW, Rathouz MM, Berg DK (1992) Nicotinic receptors that bind α-bungarotoxin on neurons raise intracellular free Ca^{2+}. Neuron 8:353–362.

Woolsey TA, Van der Loos H (1970) The structural organization of layer IV in the somatosensory regions (S1) of mouse cerebral cortex: the description of a cortical field composed of discrete cytoarchitectonic units. Brain Res 17:205–242.

Zhang ZW, Vijayaraghavan S, Berg DK (1994) Neuronal acetylcholine receptors that bind α-bungarotoxin with high affinity function as ligand-gated ion channels. Neuron 12:167–177.